

Article

An Improved Approach for Estimating Daily Net Radiation over the Heihe River Basin

Bingfang Wu ^{*}, Shufu Liu, Weiwei Zhu, Nana Yan, Qiang Xing and Shen Tan

Institute of Remote Sensing and Digital Earth (RADI), Chinese Academy of Sciences, Beijing 100094, China; liusf01@radi.ac.cn (S.L.); zhuww@radi.ac.cn (W.Z.); yan@radi.ac.cn (N.Y.); xingqiang@radi.ac.cn (Q.X.); tanshen@radi.ac.cn (S.T.)

* Correspondence: wubf@radi.ac.cn; Tel.: +86-10-6485-5689; Fax: +86-10-6485-8721

Academic Editor: Jason K. Levy

Received: 27 September 2016; Accepted: 29 December 2016; Published: 4 January 2017

Abstract: Net radiation plays an essential role in determining the thermal conditions of the Earth's surface and is an important parameter for the study of land-surface processes and global climate change. In this paper, an improved satellite-based approach to estimate the daily net radiation is presented, in which sunshine duration were derived from the geostationary meteorological satellite (FY-2D) cloud classification product, the monthly empirical a_s and b_s Angstrom coefficients for net shortwave radiation were calibrated by spatial fitting of the ground data from 1997 to 2006, and the daily net longwave radiation was calibrated with ground data from 2007 to 2010 over the Heihe River Basin in China. The estimated daily net radiation values were validated against ground data for 12 months in 2008 at four stations with different underlying surface types. The average coefficient of determination (R^2) was 0.8489, and the averaged Nash-Sutcliffe equation (NSE) was 0.8356. The close agreement between the estimated daily net radiation and observations indicates that the proposed method is promising, especially given the comparison between the spatial distribution and the interpolation of sunshine duration. Potential applications include climate research, energy balance studies and the estimation of global evapotranspiration.

Keywords: daily net radiation; sunshine duration; cloud classification; FY-2D; Heihe River Basin

1. Introduction

Net radiation (R_n) is the balance between the downward and upward shortwave and longwave radiation and is a key component of the Earth's surface energy balance. It is the main source of energy for the physical and chemical processes that occur in the surface-atmosphere interface, the heat and water budgets, photosynthesis [1] and evapotranspiration [2], which are used as input for global and regional climate change and eco-hydrological models. Net radiation especially affects the energy balance closure and the accuracy of evapotranspiration estimation algorithms [3,4]; therefore, the accurate estimation of net radiation is important for researchers in the fields of meteorology, hydrology, global change and agriculture [5–7].

Net radiation can be reliably obtained using net radiometers or shortwave and longwave radiometers, and it is routinely recorded at meteorological and radiation stations. Although such instruments are accurate for measuring net radiation at a station (representative for a certain area), their use for large regional net radiation assessments is time consuming and expensive because numerous ground installations are required, especially when large spatial coverage and a high sampling frequency are desired. Net radiation is not measured directly in most national basic meteorological stations due to restrictions imposed by economic and technical conditions, unless the station is required for radiation studies. In addition, few national radiation stations exist, resulting in insufficient net radiation data in some areas.

Various methods have been recommended for obtaining net radiation on a regional scale. Currently, the most commonly used methods for calculating net radiation are applied to the calculation of net shortwave and net longwave radiation. Net shortwave radiation is obtained by using the surface albedo and global solar radiation. The surface albedo can be calculated from remote sensing data using different band reflectances [8]. Global solar radiation can be obtained by several empirical models involving various climatic variables, including extra-terrestrial solar radiation, sunshine duration, mean temperature, maximum temperature, minimum temperature, water saturation deficit, soil temperature, the number of rainy days, altitude, latitude, total precipitation, the Sun-Earth distance, and the Julian day [9–37]. The most widely used method is the Angstrom-Prescott model, which has been applied in many countries [24,38–43] in various forms, such as quadratic, third degree, logarithmic and exponential forms. The Angstrom-Prescott model and its revised variants most commonly use sunshine duration for estimating global solar radiation. According to the comparative study by Can and Oman [44] and Kadir [35], global solar radiation models based on sunshine duration could give more accurate results than those based on other meteorological variables without sunshine duration. Although sunshine duration can be obtained from ground measurements, their application to regional and global solar radiation calculations suffers from the limited availability of ground data. Robaa [45] developed an empirical method based on the amount of clouds to estimate sunshine duration, in which empirical equations were proposed based on relative sunshine duration and readily available cloud amount data from Moderate Resolution Imaging Spectroradiometer (MODIS). This method does not consider the changes in the cloud amount between sunrise and sunset, and it can calculate only monthly sunshine duration, not daily sunshine duration. Wu et al. [46] proposed a new method to derive sunshine duration from geostationary meteorological satellite hourly cloud classification data based on a new index—the cloud classification coverage-type sunshine factor—and this method can accurately estimate daily sunshine duration without ground measurements.

In addition to sunshine duration, the empirical Angstrom a_s and b_s coefficients are needed to calculate global solar radiation using the original and revised variants of the Angstrom-Prescott model. Common values of these coefficients range between 0 and 1 (0.25 and 0.5 have been recommended when no ground measurements are available for calibration). The former expresses the fraction of extra-terrestrial radiation reaching the ground on an overcast day ($n = 0$) and depends on the atmospheric conditions (humidity and aerosols) and the solar angle [9,35,47]. Ground measurements are commonly used to fit the values of a_s and b_s , and several researchers [36,48–51] have estimated these coefficients on an annual scale in different regions. However, using a fixed coefficient on an annual scale is not appropriate for our purposes because of the regional environmental characteristics, and thus, the monthly empirical Angstrom coefficient should be fitted. Zhao et al. [37] suggested a new approach based on Air Pollution Index (API) data from ground measurements to adjust the Angstrom coefficients. Because of the limited number of ground stations and the short site observation time, this method has high precision but is not generalizable. Therefore, ground-measured radiation and meteorological data can be fully utilized to fit the monthly empirical Angstrom coefficients a_s and b_s , which is a better method to estimate global solar radiation based on sunshine duration data.

Meteorological variables are commonly used to estimate net longwave radiation: water vapour pressure, air temperature, and downward shortwave radiation or sunshine duration, as in the Food and Agricultural Organization of the United Nations (FAO)-56 Penman equation [17,27,52]. The daily net longwave radiation equation coefficients based on the FAO-56 Penman equation have been applied to various situations in many countries and regions. However, it must be calibrated with local ground measurements [47,53–55], and the downward shortwave radiation and sunshine duration required in the calibration process can be calculated based on geostationary meteorological satellite hourly cloud classification data.

The objective of this study was to investigate an improved method to derive daily net radiation based on remote sensing products coupled with field measurement data. We focused on calculating global solar radiation based on sunshine duration from Feng-Yun (FY)-2D geostationary meteorological

satellite data using the method described by Wu et al. [46], monthly a_s and b_s Angstrom coefficients based data from radiation stations, and the calibration of daily net longwave radiation based on ground measurements. The estimated daily net radiation values from this proposed algorithm were validated with independent ground observation data, and the spatial distribution was compared with the results of net radiation based on the sunshine duration using meteorological station data interpolation.

2. Methodology

2.1. Study Area

The Heihe River Basin, located in the northwest region of China between $97^{\circ}24' E$ – $102^{\circ}10' E$ and $37^{\circ}41' N$ – $42^{\circ}42' N$, is the second largest inland river basin in China, covering an area of approximately 143,000 km². Its elevation ranges from approximately 5000 m in the upper reaches to 1000 m downstream. The river originates in the Qilian mountains and flows through the Hexi corridor of Gansu Province from the Yingluo Gorge, through the Zhengyi Gorge, and then northward into the Ejina oasis in the western part of the Inner-Mongolia Plateau, before finally discharging into the east and west Juyan lakes (Figure 1). The landscape varies from glaciers and frozen soil to alpine meadow, forest, irrigated cropland, riparian ecosystems, bare Gobi, and desert. A large proportion of the watershed area comprises sparse vegetation or bare land. The highest air temperatures are approximately 40 °C downstream in the summer, and the lowest are approximately –40 °C in the upper watershed in winter. The mean annual rainfall across the basin is 110 mm·year^{−1} (1980–2010) [56], and the annual precipitation in the upstream area is more than 350 mm·year^{−1}, it is 100–250 mm·year^{−1} in the middle reaches, and the annual precipitation in the downstream area is less than 50 mm·year^{−1}.

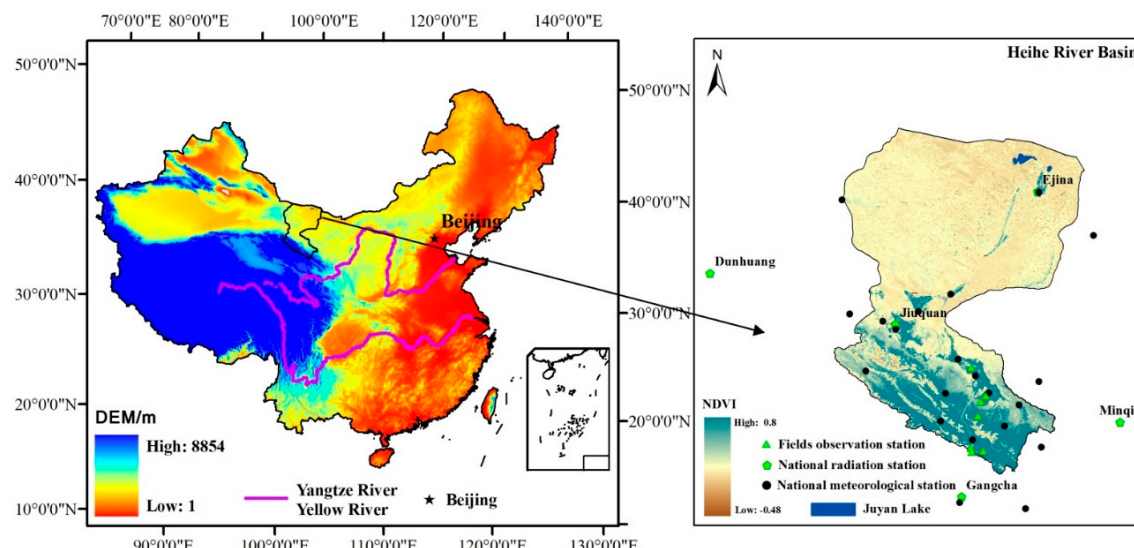


Figure 1. Location and physiography of the Heihe River Basin.

Because of the scarce water resources in this basin, a large number of hydrology and water resources, environmental ecology, and land surface process research projects have been conducted in the region since 1989, such as Heihe Basin Field Experiment (HEIFE) [57,58], Arid Environment Comprehensive Monitoring Plan '95 (AECMP '95) [59], DunHuang Experiment (DHEX) [60], the Watershed Allied Telemetry Experimental Research (WATER) project [61], and the Heihe WATER (HiWATER) project [62]. A large body of ground observation data from meteorological, hydrological and energy flux stations and associated study results has been accumulated. This rich knowledge resource has laid the foundation for much of the scientific research in the Heihe River Basin, and also the high heterogeneity of the underlying surface and the strong seasonal weather changes in the Heihe River Basin can better test the feasibility of the new method proposed in this paper.

2.2. Data and Process

2.2.1. Field Observation Data

The field observation data include radiation and meteorological data obtained during the WATER experiments [61], which can be downloaded from <http://westdc.westgis.ac.cn>. The observation stations involved in the WATER experiments are described in Table 1. Yingke station was installed in the central area of the oasis, which is located within typical irrigated farmland on which maize and wheat are grown. Linze station was installed in the grassland ecological experimental station of Lanzhou University in Linze County on typical wetland and saline alkali land. Huazhaizi station was installed on the desert beach in the southern city of Zhangye in a typical bare Gobi landscape in the middle reaches of the Heihe River Basin. Arou, Yakou, Binggou and Maliantan stations are representative of the upper reaches of the Heihe River Basin, which consist of typical alpine meadow and sparse grass. An automatic meteorological observation system and a radiation observation system were installed at each site to obtain the air temperature, air humidity, wind speed, wind direction, air pressure, precipitation, soil temperature and the soil moisture profile, solar radiation, upward short-wave radiation, upward long-wave radiation, downward long-wave radiation and soil heat flux data. Quality control for all ground measurements was performed by the data suppliers. Observation data from Yakou, Binggou and Huazhaizi stations from 2007 to 2010 and from Yingke, Linze, Arou and Maliantan stations in 2007, 2009 and 2010 were used to calibrate the parameters of the proposed net longwave radiation model. The remaining 2008 observations from Yingke, Linze, Arou and Maliantan stations were used for model validation.

Table 1. Field observation station information for the Heihe River Basin.

Station Name	Longitude (°, E)	Latitude (°, N)	Elevation (m)	Land Cover	Observation Period	Location
Huazhaizi	100.32	38.77	1731	Bare Gobi	2008.06–2010.12	Midstream
Yingke	100.41	38.86	1519	Maize	2007.11–2010.12	Midstream
Arou	100.46	38.04	3033	Alpine meadow	2007.07–2010.12	Upstream
Linze	100.07	39.25	1394	Grass	2007.10–2008.10	Midstream
Maliantan	100.30	38.55	2817	Sparse grass	2007.11–2009.12	Upstream
Yakou	100.24	38.01	4147	Alpine meadow	2007.10–2009.10	Upstream
Binggou	100.22	38.07	3449	Sparse grass	2007.9–2009.9	Upstream

2.2.2. MODIS and FY-2D Satellite Data

The MODIS 1B clear-sky data covering the Heihe River Basin were collected for 2007 to 2010. We performed a geometric correction using the built-in Ground Control Point (GCP) of the image and calculated the reflectance or radiance, which provided the calibration coefficients. We determined the cloud pixels using a method proposed by Ackerman et al. [63] that separates clear pixels from cloud-contaminated pixels using threshold values with multiple characteristics. The normalized difference vegetation index (NDVI) in the experimental area was calculated using the MODIS 1 2-band reflectivity after atmospheric correction, and the leaf area index (LAI) was calculated from the NDVI [64]. The surface albedo was computed based on a linear combination of the first seven reflectance bands [8].

FY-2D cloud data were generated by the FY-2D geostationary meteorological satellite at a resolution of 5 km [65,66]. Hourly FY-2D cloud classification products covering the Heihe River Basin from 2007 to 2010 were obtained (35,064 images) from the China Meteorological Administration (CMA) in Hierarchical Data Format (HDF). The hourly cloud classification coverage-type (cloud-type) data for the Heihe River Basin in a geographic projection were obtained based on a geographic lookup table (GLT) file downloaded from the National Satellite Meteorological Center (NSMC) [46].

2.2.3. Meteorological and Radiation Data from National Stations

Daily radiation data from the national radiation stations (Figure 1 and Table 2) covering the Heihe River Basin and the surrounding area from 1997 to 2006 were provided by the China National Meteorological Bureau and included sunshine duration, solar irradiation, net radiation, diffuse irradiation, horizontal direct beam irradiation, reflected radiation and vertical direct beam irradiation.

Table 2. National radiation station information for the Heihe River Basin.

Station Name	Longitude ($^{\circ}$, E)	Latitude ($^{\circ}$, N)	Elevation (m)	Land Cover	Observation Period	Location
Ejin Banner	101.07	41.95	941	Sparse forests	1997–2006	Downstream
Dunhuang	94.68	40.15	1139	Sparse forests	1997–2006	Midstream (outside)
Jiuquan	98.48	39.77	1477	Farmland	1997–2006	Midstream
Minqin	103.08	38.63	1367	Urban	1997–2006	Midstream
Gangcha	100.13	37.33	3302	Bare	1997–2006	Upstream (outside)

Daily meteorological data from 21 meteorological stations (Figure 1) covering the Heihe River Basin and the surrounding area from 2007 to 2010 were also provided by the China National Meteorological Bureau, including the maximum air temperature, minimum temperature and air humidity. To calculate the net radiation, all variables were interpolated into a daily map at a resolution of 1 km. Squared inverse distance weighting was used for air temperature interpolation, in combination with digital elevation model (DEM) data, and thin plate splines were employed for air humidity interpolation [67].

All the daily radiation and meteorological data used in this paper were provided by the China Meteorological Data Center and can be downloaded from http://cdc.cma.gov.cn/cdc_en/home.dd. Quality control of the data was performed by the suppliers.

2.3. Modelling Daily Net Radiation

The energy balance of a land surface can be described as:

$$R_n = R_{sd} - R_{su} + R_{ld} - R_{lu} \quad (1)$$

where R_n is the net radiation ($\text{MJ} \cdot \text{m}^{-2} \cdot \text{d}^{-1}$), R_{sd} is the downwelling shortwave radiation ($\text{MJ} \cdot \text{m}^{-2} \cdot \text{d}^{-1}$), R_{su} is the upwelling shortwave radiation ($\text{MJ} \cdot \text{m}^{-2} \cdot \text{d}^{-1}$), R_{ld} is the downwelling longwave radiation ($\text{MJ} \cdot \text{m}^{-2} \cdot \text{d}^{-1}$), and R_{lu} is the upwelling longwave radiation ($\text{MJ} \cdot \text{m}^{-2} \cdot \text{d}^{-1}$). Alternatively, R_n is the sum of the daily net shortwave radiation and the daily net longwave radiation and can be written as:

$$R_n = R_{ns} + R_{nl} \quad (2)$$

where R_{ns} is the net shortwave radiation ($\text{MJ} \cdot \text{m}^{-2} \cdot \text{d}^{-1}$), and R_{nl} is the net longwave radiation ($\text{MJ} \cdot \text{m}^{-2} \cdot \text{d}^{-1}$). The net shortwave radiation can be calculated from the global solar irradiation (R_s) and the surface albedo (α) as:

$$R_{ns} = R_s(1 - \alpha) \quad (3)$$

The surface albedo can be computed from a linear combination of the first seven reflectance bands based on MODIS data. If the global solar irradiation and daily net longwave radiation are known, the daily net radiation can be estimated on a regional scale by combining Equations (2) and (3).

2.3.1. Global Solar Radiation

The most widely used method to estimate global solar radiation is the Angstrom-Prescott model [9,68,69]:

$$R_s = \left(a_s + b_s \frac{n}{N} \right) R_a \quad (4)$$

where R_s and R_a are the global solar radiance ($\text{MJ} \cdot \text{m}^{-2} \cdot \text{d}^{-1}$) and extra-terrestrial solar irradiance ($\text{MJ} \cdot \text{m}^{-2} \cdot \text{d}^{-1}$), respectively; n stands for the actual sunshine duration of bright sunshine (h); N is the maximum possible sunshine duration (h); and a_s and b_s are empirically determined regression coefficients.

The following equation combines the new index cloud-type factor [46], which is shown in Table 3. The hourly FY-2D cloud type product mentioned in Section 2.2.2 as used to estimate the daily sunshine duration (n) with a resolution of 1 km over the Heihe River Basin:

$$FY_{sunt} = \sum_{i=h_{sr}+0.25}^{i=h_{ss}-0.25} SF_i \times T_{gap} \quad (5)$$

where FY_{sunt} stands for the sunshine duration (between 15 min (+0.25 h) after the start of sunrise and 15 min (-0.25 h) before sunset and the accumulation of sunshine factors); SF is the FY-2D cloud cover-type factor (Table 3), which is the index for the hourly FY-2D hourly cloud type data from sunrise to sunset; T_{gap} is an hour's interval with a value of 1; i is the time series that ranges between sunrise and sunset at the local time; and h_{sr} and h_{ss} are the times of sunrise time and sunset, respectively, and can be calculated from the latitude and solar declination based on the day of the year.

Table 3. FY-2D cloud-type factor for the Heihe River Basin.

Code	Cloud Type (Cloud Classification)	Factor
0/1	Clear Sky	0.9
11	Mixed pixels	0.21
12	Altostratus or Nimbostratus	0.25
13	Cirrostratus	0.51
14	Cirrus spissatus	0.24
15	Cumulonimbus	0.13
21	Stratocumulus or Altocumulus	0.35

The extra-terrestrial solar irradiance R_a ($\text{MJ} \cdot \text{m}^{-2} \cdot \text{d}^{-1}$) is calculated as follows:

$$R_a = \frac{24 \times 60}{\pi} G_{sc} d_r [\omega_s \sin(\varphi) \sin(\delta) + \cos(\varphi) \cos(\delta) \sin(\omega_s)] \quad (6)$$

where G_{sc} is the solar constant ($0.082 \text{ MJ} \cdot \text{m}^{-2} \cdot \text{min}^{-1}$), d_r is the inverse relative distance between the Earth and the Sun, φ is the latitude (radians), δ is the solar declination (radians), and ω_s is the sunset hour angle (radians). The values of d_r and δ can be calculated with Equations (7) and (8):

$$d_r = 1 + 0.033 \cos\left(\frac{2\pi}{365} J\right) \quad (7)$$

$$\delta = 0.409 \sin\left(\frac{2\pi}{365} J - 1.39\right) \quad (8)$$

where J is the Julian day (the day of the year) between 1 January and 31 December ($J = 1, \dots, n$; $n = 365$ or 366). The parameter ω_s is calculated with φ and δ as:

$$\omega_s = \arccos[-\tan(\varphi) \tan(\delta)] \quad (9)$$

The maximum possible sunshine duration, N in Equation (4), is calculated as follows:

$$N = \frac{24}{\pi} \omega_s \quad (10)$$

Based on the actual sunshine duration from the hourly FY-2D cloud type and Equation (5), Equation (4) can be used to calculate the regional daily global solar radiation over the Heihe River Basin, provided the regression a_s and b_s Angstrom coefficients are known. Daily radiation records (1997–2006) for the stations in Table 2 were used to compute the Angstrom coefficients, which were subsequently spatially interpolated and combined with daily sunshine duration from the hourly FY-2D cloud type based on the Equation (5).

2.3.2. Net Longwave Radiation

When using the FAO-56 Penman method, the net longwave radiation (R_{nl} , $\text{MJ} \cdot \text{m}^{-2} \cdot \text{d}^{-1}$) is calculated by determining the net longwave radiation for a clear sky, which has been improved by various researchers [47,53,70,71] for cloud cover conditions. The equation can be written as:

$$R_{nl} = \sigma \frac{T_{\max}^4 + T_{\min}^4}{2} \varepsilon_{net} f_{cloudiness} \quad (11)$$

where σ is the Stefan-Boltzmann constant ($\text{MJ} \cdot \text{m}^{-2} \cdot \text{d}^{-1} \cdot \text{K}^{-4}$); T_{\max}^4 and T_{\min}^4 are the daily maximum and daily minimum air temperatures at a height of 2 m (K), respectively; ε_{net} is the net emissivity; and $f_{cloudiness}$ is the cloudiness factor. The value of ε_{net} is calculated as the emissivity of vegetation (ε_{vs}) minus the atmospheric emissivity (ε_a) using the following equation:

$$\varepsilon_{net} = \varepsilon_{vs} - \varepsilon_a \quad (12)$$

The factor ε_{vs} is commonly calculated using the LAI. According to Bastiaanssen [72], the formula used for this calculation is as follows:

$$\varepsilon_{vs} = 0.95 + 0.01LAI, \text{ when } LAI < 3 \quad (13)$$

$$\varepsilon_{vs} = 0.98, \text{ when } LAI \geq 3 \quad (14)$$

The value of ε_a is obtained by applying the Brunt equation [70]:

$$\varepsilon_a = a_1 + b_1 \sqrt{e_a} \quad (15)$$

where a_1 and b_1 are coefficients, and e_a is the water vapour pressure (kPa). The cloudiness factor is [52]:

$$f_{cloudiness} = c_1 \frac{n}{N} + d_1 \quad (16)$$

or:

$$f_{cloudiness} = c_2 \frac{R_s}{R_{so}} + d_2 \quad (17)$$

with:

$$R_{so} = (a_s + b_s) R_a \quad (18)$$

$$c_2 = c_1 \times \frac{a_s + b_s}{b_s} \quad (19)$$

$$d_2 = -c_1 \times \frac{a_s}{b_s} + d_1 \quad (20)$$

where c_1 , c_2 , d_1 and d_2 are coefficients, and R_{so} is the clear sky solar radiation ($\text{MJ} \cdot \text{m}^{-2} \cdot \text{d}^{-1}$). Penman [71] and Jensen [53] suggest that $c_1 = 0.9$ and $d_1 = 0.1$. Allen [47] applied Equation (17) with $c_2 = 1.35$ and $d_2 = -0.35$, which were obtained by substituting the empirical a_s and b_s coefficients ($a_s = 0.25$ and $b_s = 0.50$) into Equation (4) and Equation (18) into Equation (16) using the values of empirical coefficients suggested by Penman [71] and Jensen [53].

In this study, Equation (17) has been adopted for the cloudiness factor. The empirical coefficients (c_2 and d_2) are fitting parameters, which are obtained using Equations (11)–(20) with ground observations from the Yakou, Binggou and Huazhaizi stations from 2007 to 2010 and the Yingke, Linze, Arou and Maliantan stations in 2007, 2009 and 2010. The values of a_s and b_s were obtained as indicated in Section 2.3.1. The optimal sum of c_2 and d_2 is 1.0.

In this paper, the three calibration methods described by Hiroyuki [52] were used to calibrate the parameters a_1 , b_1 , c_2 and d_2 . First, the two coefficients (a_1 and b_1) in Equation (15) are calibrated to minimize the root-mean-square error (RMSE) of the estimated longwave downward radiation when the relative sunshine duration value exceeds 0.95 (step 1). Then, the values of coefficients c_2 and d_2 were calculated by Equations (19) and (20) using the values of c_1 and d_1 suggested by Penman [71] and Jensen [53] (step 2). Finally, in step 3, c_2 and d_2 in Equation (17) were directly calibrated using the coefficients obtained in step 1 (a_1 and b_1) and the estimated values of a_s and b_s from Section 2.3.1 to minimize the RMSE of the estimated daily net longwave radiation with respect to the observed records. If the a_1 , b_1 , c_1 , c_2 , d_1 and d_2 coefficients are known, net longwave radiation can be estimated on a regional scale by combining Equations (11)–(20).

2.4. Model Performance Assessment

The model parameters are determined using numerical iteration methods [73]. The statistical indices used to evaluate the model performance include the coefficient of determination (R^2), the mean bias error (MBE), the mean absolute error (MAE), the RMSE, the index of agreement (d), and the Nash-Sutcliffe Equation (NSE) [74,75]. These values are defined as follows:

$$R^2 = \frac{\left[\sum_{i=1}^n (O_i - \bar{O})(P_i - \bar{P}) \right]^2}{\sum_{i=1}^n (O_i - \bar{O})^2 (P_i - \bar{P})^2} \quad (21)$$

$$MBE = n^{-1} \sum_{i=1}^n (P_i - O_i) \quad (22)$$

$$MAE = n^{-1} \sum_{i=1}^n |P_i - O_i| \quad (23)$$

$$RMSE = \sqrt{n^{-1} \sum_{i=1}^n (P_i - O_i)^2} \quad (24)$$

$$d = 1 - \frac{\sum_{i=1}^n (P_i - O_i)^2}{\sum_{i=1}^n (|P_i - \bar{O}| + |O_i - \bar{O}|)^2} \quad (25)$$

$$NSE = 1 - \frac{\sum_{i=1}^n (O_i - P_i)^2}{\sum_{i=1}^n (O_i - \bar{O}_i)^2} \quad (26)$$

where O_i is the actual measurement, and P_i is its estimate; \bar{O} is the mean measurement; \bar{P} is the mean of the estimates; and n is the sample size. The ideal values of the statistical tests, such as the MAE and RMSE, are 0 or close to 0. A model is more efficient when the NSE, R^2 and d values are closer to 1 [76]. Fox [77] and Willmott [78] also suggest the following: (1) The model should perform well when the MAE is less than 50% of the measured standard deviation; and (2) higher values of d are correlated with better model performance.

3. Results

3.1. Monthly Angstrom Coefficients

The monthly Angstrom coefficients a_s and b_s at five national radiation stations were estimated as the regression coefficients of the long-term monthly average radiation and sunshine duration (1997–2006) per Equation (4), and the results are listed in Table 4. The highest coefficient of determination (R^2) between the estimated solar radiation based on those regression monthly Angstrom coefficients and the observed solar radiation is 0.98, and the averaged value is 0.93. The average values of the coefficients a_s and b_s are 0.23 and 0.53, respectively; a_s varies between 0.16 and 0.36, while b_s varies from 0.44 to 0.62. The average value of a_s is less than and that of b_s is larger than the values reported by Angstrom [9] and Chen [32]. The above results indicate no obvious difference in the accuracy of the estimation of solar radiation in the low-latitude and high-latitude areas based on the monthly Angstrom coefficients. According to the monthly Angstrom coefficients at each station, the spatially distributed a_s and b_s can be obtained by spatial interpolation (inverse distance weighting with exponent 2).

Table 4. Monthly regression Angstrom coefficients of a_s and b_s at five national radiation stations.

Station	Month	R^2	a_s	b_s	Station	Month	R^2	a_s	b_s
Ejin Banner	1	0.88	0.27	0.49	Jiuquan	7	0.98	0.21	0.47
Ejin Banner	2	0.96	0.28	0.47	Jiuquan	8	0.94	0.23	0.50
Ejin Banner	3	0.94	0.25	0.45	Jiuquan	9	0.97	0.24	0.56
Ejin Banner	4	0.95	0.23	0.51	Jiuquan	10	0.92	0.22	0.52
Ejin Banner	5	0.96	0.25	0.55	Jiuquan	11	0.95	0.25	0.54
Ejin Banner	6	0.92	0.24	0.47	Jiuquan	12	0.96	0.21	0.51
Ejin Banner	7	0.98	0.23	0.54	Minqin	1	0.98	0.21	0.52
Ejin Banner	8	0.97	0.22	0.56	Minqin	2	0.92	0.20	0.51
Ejin Banner	9	0.91	0.20	0.52	Minqin	3	0.94	0.19	0.52
Ejin Banner	10	0.95	0.22	0.57	Minqin	4	0.94	0.24	0.54
Ejin Banner	11	0.91	0.26	0.53	Minqin	5	0.93	0.17	0.59
Ejin Banner	12	0.94	0.25	0.55	Minqin	6	0.89	0.19	0.51
Dunhuang	1	0.97	0.24	0.51	Minqin	7	0.88	0.24	0.56
Dunhuang	2	0.89	0.16	0.55	Minqin	8	0.94	0.24	0.54
Dunhuang	3	0.89	0.22	0.58	Minqin	9	0.93	0.23	0.58
Dunhuang	4	0.92	0.21	0.51	Minqin	10	0.89	0.24	0.59
Dunhuang	5	0.89	0.23	0.57	Minqin	11	0.90	0.18	0.58
Dunhuang	6	0.92	0.21	0.54	Minqin	12	0.91	0.21	0.51
Dunhuang	7	0.95	0.18	0.54	Gangcha	1	0.93	0.23	0.53
Dunhuang	8	0.93	0.24	0.55	Gangcha	2	0.91	0.24	0.62
Dunhuang	9	0.92	0.28	0.56	Gangcha	3	0.89	0.34	0.48
Dunhuang	10	0.90	0.23	0.48	Gangcha	4	0.93	0.36	0.54
Dunhuang	11	0.91	0.21	0.49	Gangcha	5	0.88	0.21	0.54
Dunhuang	12	0.90	0.23	0.52	Gangcha	6	0.89	0.24	0.56
Jiuquan	1	0.98	0.21	0.54	Gangcha	7	0.92	0.23	0.62
Jiuquan	2	0.98	0.22	0.52	Gangcha	8	0.89	0.30	0.55
Jiuquan	3	0.90	0.19	0.44	Gangcha	9	0.91	0.21	0.59
Jiuquan	4	0.95	0.27	0.55	Gangcha	10	0.93	0.23	0.48
Jiuquan	5	0.93	0.21	0.49	Gangcha	11	0.89	0.21	0.51
Jiuquan	6	0.96	0.20	0.54	Gangcha	12	0.88	0.21	0.59

3.2. Validation of the Global Solar Radiation

The annual Angstrom coefficients a_s and b_s at five national radiation stations were also estimated as the regression coefficients of the long-term annual average radiation and sunshine duration (1997–2006) per Equation (4). The same spatial interpolation method (inverse distance weighting with exponent 2)

was used to obtain the spatially distributed of annual a_s and b_s based on the annual Angstrom coefficients data at each station.

Two typical national radiation stations were randomly selected. The ground measurement data from these two stations in 2008 (366 days) were used to compare the estimates of daily global solar radiation determined using Equation (4) based on the spatial data of the monthly Angstrom coefficients and annual Angstrom coefficients, and also daily sunshine duration calculated from hourly FY-2D cloud-type data. Table 5 and Figure 2 show the validation results for the estimation of the daily global solar radiation and the ground measurement global solar radiation at two national radiation stations in 2008. Compared to the validation results between estimated global daily solar radiation based on the annual Angstrom coefficients and the observed values, the coefficients of determination (R^2) between the observed and estimated values from monthly Angstrom coefficients have a higher value, which were 0.9597 at Jiuquan and 0.9614 at Ejin Banner, indicating more strong correlation between the observed daily global solar radiation and the estimated daily global solar radiation from monthly Angstrom coefficients; the index of agreement (d) and NSE were 0.9873 and 0.9541 at Jiuquan and 0.9894 and 0.9588 at Ejin Banner, respectively. The higher d and NSE indicate that daily global solar radiation estimated by the proposed method correlates better with the in situ daily global solar radiation. The MBE , MAE and $RMSE$ at these two stations were $-0.1849 \text{ MJ} \cdot \text{m}^{-2} \cdot \text{d}^{-1}$, $1.2432 \text{ MJ} \cdot \text{m}^{-2} \cdot \text{d}^{-1}$, $1.6419 \text{ MJ} \cdot \text{m}^{-2} \cdot \text{d}^{-1}$, and $-0.3860 \text{ MJ} \cdot \text{m}^{-2} \cdot \text{d}^{-1}$, $1.1291 \text{ MJ} \cdot \text{m}^{-2} \cdot \text{d}^{-1}$, $1.4946 \text{ MJ} \cdot \text{m}^{-2} \cdot \text{d}^{-1}$, respectively. The relativized magnitude of MBE is from $5.9945 \text{ MJ} \cdot \text{m}^{-2} \cdot \text{d}^{-1}$ to $5.3658 \text{ MJ} \cdot \text{m}^{-2} \cdot \text{d}^{-1}$ at Jiuquan and from $-3.1381 \text{ MJ} \cdot \text{m}^{-2} \cdot \text{d}^{-1}$ to $6.3227 \text{ MJ} \cdot \text{m}^{-2} \cdot \text{d}^{-1}$ at Ejin Banner. The lower MAE and $RMSE$ values between the observed and the estimated values by the proposed method than the results by the annual Angstrom coefficients suggest that few outliers are present in the estimated daily global solar radiation values.

Table 5. Statistics for the performance of the global daily solar radiation estimated by the proposed method at Jiuquan and Ejin Banner stations in 2008 (366 days).

Station	Angstrom Coefficients	Time	R^2	MBE $\text{MJ} \cdot \text{m}^{-2} \cdot \text{d}^{-1}$	MAE $\text{MJ} \cdot \text{m}^{-2} \cdot \text{d}^{-1}$	$RMSE$ $\text{MJ} \cdot \text{m}^{-2} \cdot \text{d}^{-1}$	d	NSE
Jiuquan	Monthly	2008.1.1–2008.12.31	0.9597	-0.1849	1.2432	1.6419	0.9873	0.9541
	Annual	2008.1.1–2008.12.31	0.9202	-0.8533	1.5853	2.3920	0.9723	0.9026
Ejin Banner	Monthly	2008.1.1–2008.12.31	0.9614	-0.3860	1.1291	1.4946	0.9894	0.9588
	Annual	2008.1.1–2008.12.31	0.9196	0.1035	1.5692	2.1187	0.9769	0.9172

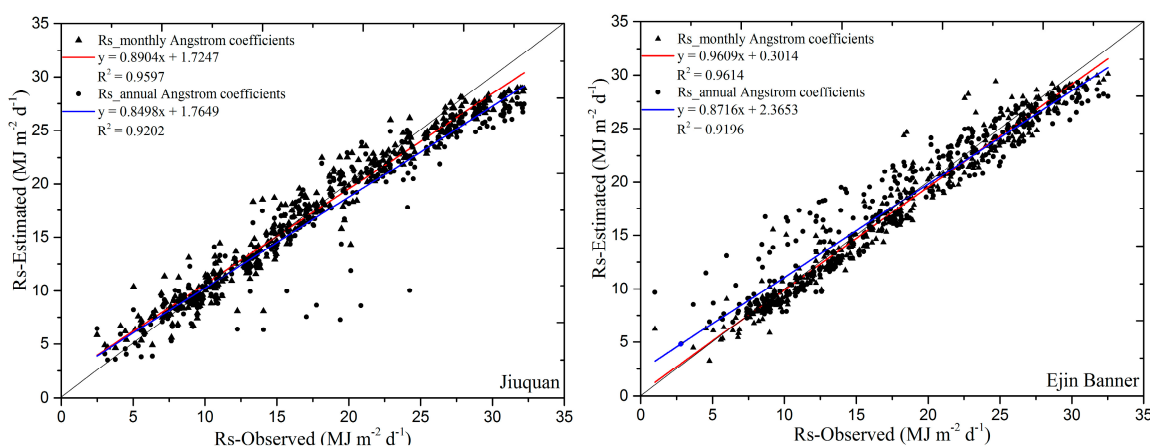


Figure 2. Comparison of the observed and estimated global daily solar radiation in 2008 (366 days) at Jiuquan (left) and Ejin Banner (right).

3.3. Calibration of Net Longwave Radiation

All the observations from the Yakou, Binggou and Huazhaizi stations and the data from the Yingke, Linze, Arou and Maliantan stations in 2007, 2009 and 2010 were used to calibrate the model parameters of the proposed net longwave radiation model in Section 2.3.2. The calibration data encompassed different underlying surface types (upstream and midstream) in the Heihe River Basin. Based on Section 2.3.2, the final calibration coefficients show that a_1 , b_1 , c_1 , c_2 , d_1 and d_2 are 0.62, 0.15, 0.58, 0.84, 0.41 and 0.15, respectively. According to Equations (27) and (28), the final daily net longwave radiation equation after calibration and the comprehensive coefficients for the Heihe River Basin: $0.33 + 0.01LAI$ or $0.36 - 0.15\sqrt{e_a}$, $0.84\frac{R_s}{R_{so}} + 0.15$, for $LAI < 3$; $0.36 - 0.15\sqrt{e_a}$, $0.84\frac{R_s}{R_{so}} + 0.15$, for $LAI \geq 3$; these values are substantially different from those suggested by Allen [47] (0.34, -0.14 , 1.35 and -0.35 , respectively) and Huang et al. [50] (0.39, 0.058, 0.1, and 0.9, respectively):

$$R_{nl} = \sigma \left(\frac{T_{\max}^4 + T_{\min}^4}{2} \right) (0.33 + 0.01LAI - 0.15\sqrt{e_a}) \left(0.84 \frac{R_s}{R_{so}} + 0.15 \right), \text{ for } LAI < 3 \quad (27)$$

$$R_{nl} = \sigma \left(\frac{T_{\max}^4 + T_{\min}^4}{2} \right) (0.36 - 0.15\sqrt{e_a}) \left(0.84 \frac{R_s}{R_{so}} + 0.15 \right), \text{ for } LAI \geq 3 \quad (28)$$

3.4. Net Radiation over the Heihe River Basin

After developing the daily solar radiation method and the calibration of the daily longwave radiation, the improved net radiation equation and the final parameters can be obtained. The 2008 ground data were used to validate the estimated daily net radiation. At the same time, an inverse distance weighting (IDW) interpolation method [79] was used to estimate daily sunshine duration, which was then applied to estimate the daily net radiation based on the method proposed in this paper instead of the sunshine duration calculated by the hourly FY-2D cloud-type data. The performance of the proposed method based on the sunshine duration from hourly FY-2D cloud-type data and station interpolation method is presented in Figure 3 and Table 6. Compared to the validation results between estimated daily net radiation based on the sunshine duration from station interpolation method (Rn_Interpolation method) and the observed values, the coefficients of determination (R^2) between the observed values and the estimated values based on the sunshine duration from hourly FY-2D cloud-type data (Rn_FY-2D cloud-type) have a higher value, which were 0.8703, 0.8903, 0.9003 and 0.8489 at Arou, Yingke, Linze and Maliantan, respectively. The maximum R^2 value is 0.9003, and the average is 0.8489, indicating a strong correlation between the observed and estimated values (Rn_FY-2D cloud-type). The indexes of agreement (d) at Arou, Yingke, Linze and Maliantan are 0.9518, 0.9684, 0.9771 and 0.9231, respectively, which also suggest good performance again. The NSE values at Arou, Yingke, Linze and Maliantan are 0.8279, 0.8837, 0.9160 and 0.7147, respectively. The maximum NSE value is 0.9160, and the average value is 0.8356. The higher values of d and NSE again indicate that the daily net radiation estimated by the proposed method (Rn_FY-2D cloud-type) correlates well with the in situ daily net radiation. The MBE, MAE and RMSE values determined at these four stations show that lower MAE and RMSE values from Rn_FY-2D cloud-type than the results by the Rn_Interpolation method are correlated with the existence of fewer outliers in the estimated daily net radiation values.

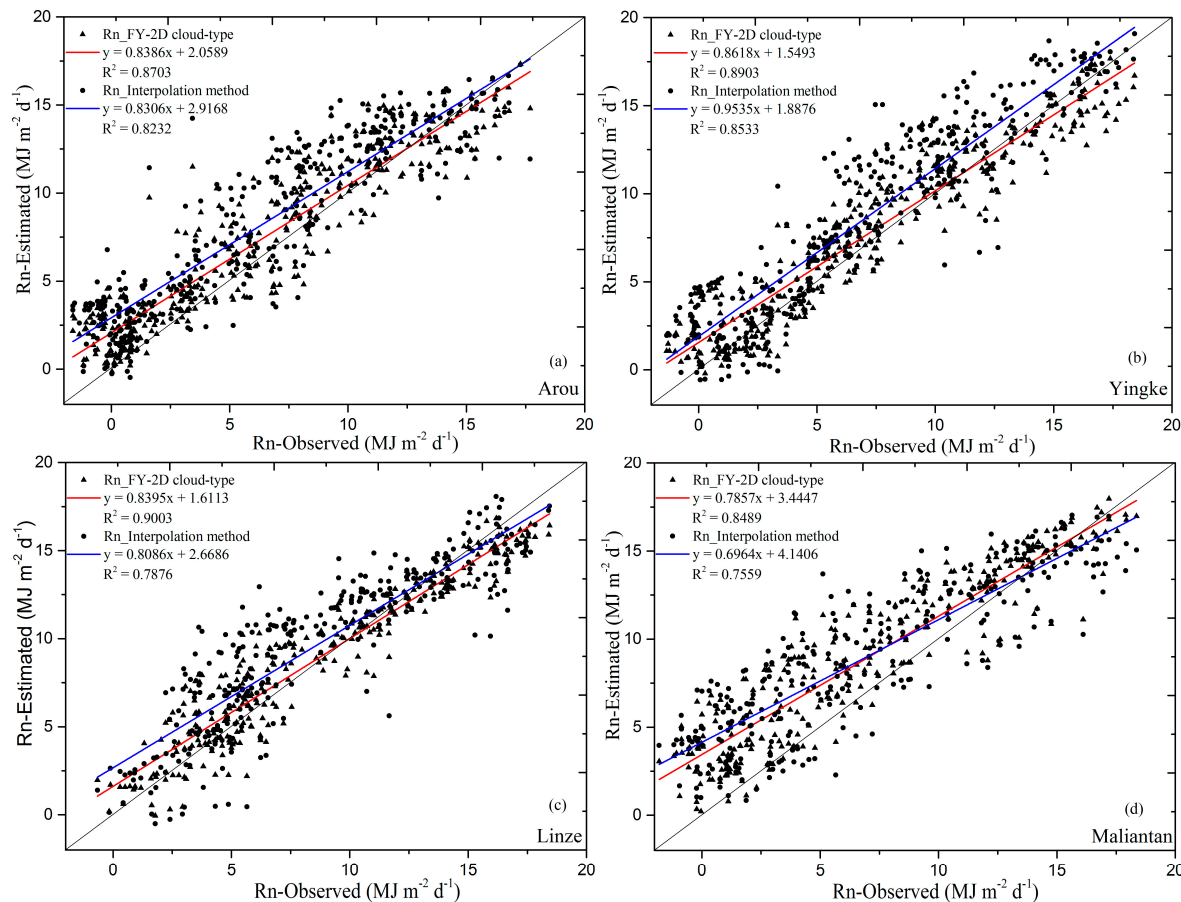


Figure 3. Comparison of the observed and estimated daily net radiation in 2008 (366 days) at Arou (a); Yingke (b) Linze (c) and Maliantan (d) stations.

Table 6. Statistics for the performance of daily net radiation estimated by the proposed method at the Arou, Yingke, Linze and Maliantan stations in 2008 (366 days).

Station	Sunshine Duration	Time	R ²	MBE MJ·m ⁻² ·d ⁻¹	MAE MJ·m ⁻² ·d ⁻¹	RMSE MJ·m ⁻² ·d ⁻¹	d	NSE
Arou	FY-2D cloud-type	2008.1.1–2008.12.31	0.8703	1.0580	1.6908	2.1600	0.9518	0.8279
	Interpolation method	2008.1.1–2008.12.31	0.8232	1.8667	2.3700	2.8752	0.9172	0.6950
Yingke	FY-2D cloud-type	2008.1.1–2008.12.31	0.8903	0.5411	1.4519	1.8196	0.9684	0.8837
	Interpolation method	2008.1.1–2008.12.31	0.8533	1.5481	2.0199	2.5923	0.9454	0.7640
Linze	FY-2D cloud-type	2008.1.1–2008.12.31	0.9003	0.2162	1.2396	1.5925	0.9771	0.9160
	Interpolation method	2008.1.1–2008.12.31	0.7876	1.0041	1.9807	2.4724	0.9492	0.7975
Maliantan	FY-2D cloud-type	2008.1.1–2008.12.31	0.8489	1.9696	2.3552	2.8958	0.9231	0.7147
	Interpolation method	2008.1.1–2008.12.31	0.7559	2.0506	2.7992	3.3768	0.8892	0.6121

To explore the variation of the spatial distribution, Figure 4 compares the results for the Heihe River Basin on 16 July 2008 using the proposed method based on the sunshine duration from hourly FY-2D cloud-type data and station interpolation method. It's also gave the spatial distribution of the

difference between both methods in the Figure 4. Because meteorological stations are sparse in the upstream and downstream regions in Heihe River Basin, the difference between the two methods is obvious. Wu et al. [46] had described the spatial distribution of the sunshine duration based on the hourly FY-2D cloud-type data, in which the spatial distribution was better than by a method based on interpolation among meteorological stations data, especially in the upstream and downstream regions in Heihe River Basin due to few ground observation stations. Therefore, the method proposed in this paper based on the hourly FY-2D cloud-type data is clearly the best method to reflect the variation of the spatial distribution of the daily net radiation.

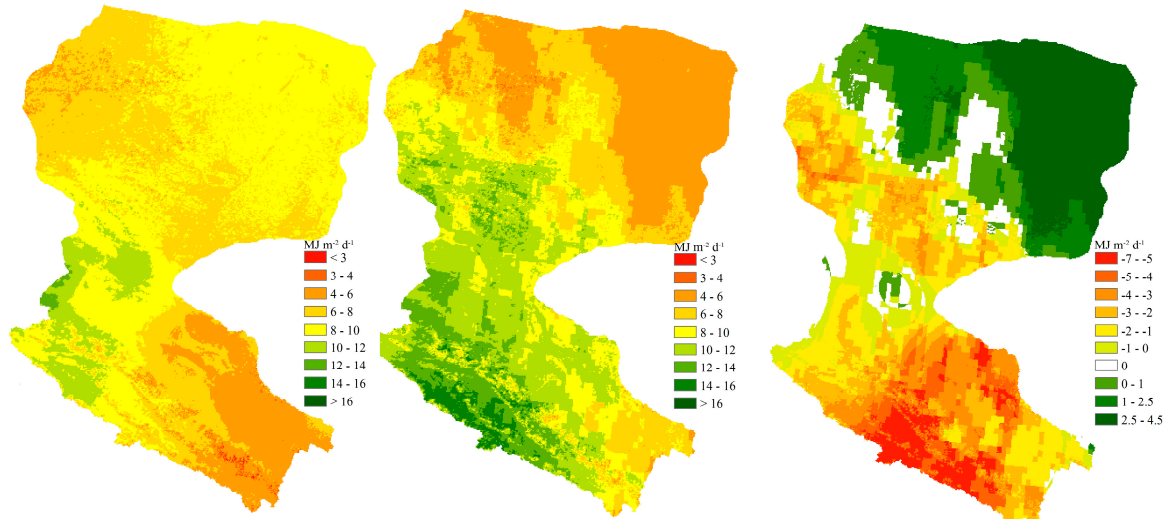


Figure 4. Spatial distribution of daily net radiation ($\text{MJ} \cdot \text{m}^{-2} \cdot \text{d}^{-1}$) estimated using sunshine duration-IDW (left); the proposed model (middle) and the difference between both methods (right) over the Heihe River Basin in 16 July 2008.

4. Discussion

Daily net radiation plays an essential role in determining the thermal conditions of the Earth's surface. It is an important variable in modelling studies of land-surface processes and global climate change. The goal of this study was to accurately and easily estimate daily net radiation based on remote sensing products coupled with field measured data. This new method has the potential to estimate daily variations of surface net radiation and evapotranspiration over large regions.

Equation (4) indicates that a positive relationship exists between sunshine duration and global solar radiation. Additionally, the accuracy of the sunshine duration calculation directly affects the accuracy of the net radiation obtained by combining Equations (2), (27) and (28). The method based on the hourly FY-2D cloud type used to estimate sunshine duration is different from the interpolation method used for the ground measurement data, and it can better express the spatial variation of sunshine duration on a regional scale without ground measurements. For the downstream Heihe River Basin in particular, because of the lack of ground observation stations indicated in Figure 1, sunshine duration based on the hourly FY-2D cloud type can significantly improve the estimation of net radiation on a spatial scale, as shown in Figure 4.

The Angstrom coefficients a_s and b_s affect the solar radiation and net radiation based on Equations (2) and (4). Because of complex changes in the atmospheric conditions (humidity and aerosols) and the solar angle, an annual coefficient does not appropriately reflect the complex atmospheric conditions, and because of the limitations of the ground measurement data, it is impossible to obtain the daily Angstrom coefficients a_s and b_s . Therefore, in this study, the monthly Angstrom coefficients were calculated instead, as shown in Table 4, and better reflect the changes in the regional atmospheric conditions used to estimate the daily global solar radiation. In addition, the estimate of

global solar radiation based on the spatial interpolation of the monthly Angstrom coefficients a_s and b_s from the ground sites was also better than that for the solar radiation based on a fixed coefficient on an annual scale, regardless of the spatial interpolation method applied.

Currently, various researchers are using different net longwave radiation estimation methods, all of which must be re-calibrated when applied to a new study site. In this paper, a set of parameters for the Heihe River Basin was calibrated for calculating net longwave radiation combined with LAI data and field measurement data. The parameter values were slightly different from those of Allen et al. [47] and Huang et al. [50] and could improve the net longwave radiation results.

Regarding the sunshine duration in mountain areas determined based on the Wu's method using hourly FY-2D cloud-type data [46], because of the effects of topography and the heterogeneity of the mountain surface, the accuracy of the sunshine duration in the mountain area was less than that in the plain area. While more human activity occurs in the lowlands than in the mountains, the modification of atmospheric environment conditions affected by human activities in the lowlands was more frequently, so the monthly Angstrom coefficients a_s and b_s may also change in other years in the plain area even if the higher accuracy of the monthly Angstrom coefficients a_s and b_s have been obtained based on the historical data. Therefore, based on the Angstrom coefficients and sunshine duration, no obvious difference in the estimation accuracy of the net radiation between the mountain and plain areas was noted from Figure 3 and Table 6.

Figure 4 compares the results of the proposed method and that based on meteorological data interpolation for the Heihe River Basin. An obvious difference between the two methods for estimating the spatial distribution of net radiation was noted. Wu et al. [46] has described the spatial distribution of the sunshine duration based on the hourly FY-2D cloud-type data, in which the spatial distribution was better than by a method based on interpolation among meteorological stations data. While the proposed method does not depend on the number of surface weather stations, the monthly Angstrom coefficients of a_s and b_s were used instead of fixed coefficients, and a set of parameters was calibrated to calculate net longwave radiation combined with LAI data and field measurement data over the Heihe River Basin. Therefore, as shown in Figure 4 and Table 6, the method proposed in this paper can better reflect the difference in the spatial distribution of daily net radiation, especially in the upstream and downstream regions.

The proposed method allows daily net radiation to be derived from remote sensing products. For cloud-type data from FY-2D, the pixel value represents the average sunshine duration for an area of $5 \text{ km} \times 5 \text{ km}$. In addition, the cloud-type data do not account for smaller clouds, which also affect the sunshine duration estimation and daily net radiation. Ground measurements of sunshine duration and net radiation represent a much smaller area, which does not correspond to the area covered by a pixel. Consequently, some outliers would be expected in Table 6 and Figure 3, in which the estimated values are compared with the measured values. However, the terrain near most ground measurement stations is relatively flat with fairly homogeneous surface coverage. Thus, the ground measurement values can be assumed to represent the average value for the surrounding region and be appropriately matched with remotely sensed pixel values.

Whether fitting the monthly angstrom coefficients a_s and b_s , calibrating net longwave radiation parameters, or optimizing the FY-2D cloud-type factors, the proposed method requires a large quantity of ground data. Therefore, calculating the net radiation on a regional scale in the absence of ground data is difficult. Fortunately, data from reanalysis products (National Centers for Environmental Prediction [NCEP], Modern Era Retrospective Analysis for Research and Applications [MERRA] and Global Land Data Assimilation System [GLDAS]) can provide hourly, 3-h, 6-h or daily radiation and meteorological data. Thus, data from reanalysis products can be used in the proposed method to replace ground data for the fitting and calibration steps to estimate net radiation on a regional scale, even if the data from those reanalysis products are of low resolution.

The accuracy of net radiation estimates, net longwave radiation calibration and the Angstrom coefficients is negatively affected by the limited number of ground stations that measure radiation and

other variables. More ground data or data from reanalysis products will be needed for model fitting and calibration to apply the proposed method in other regions.

5. Conclusions

A method was developed to derive daily net radiation based on remote sensing products coupled with field measurement data. The methodology was validated with data collected over the Heihe River Basin in northeast China in 2008. This method estimates daily global solar radiation based on sunshine duration from the FY-2D geostationary meteorological satellite, as described by Wu et al. [46]. A spatial fitting method was used to estimate the monthly a_s and b_s Angstrom coefficients based on ground radiation and meteorological data. The daily net longwave radiation was calibrated using ground data and the net longwave radiation equation. The results from this method show that the estimated daily net radiation and in situ measurements agree fairly well, confirming the soundness and good performance of the proposed method. The analysis of the spatial distribution of daily net radiation shows that the new method represents sunshine fields better than the interpolation of sunshine data.

Acknowledgments: This work was supported in part by Advanced Science Foundation Research Project of the Chinese Academy of Sciences (Grant No. QYZDY-SSW-DQC014) and part by the Natural Science Foundation of China, Grant No. 41271424 and No. 91025007. The geostationary meteorological satellite data (FY-2D) were provided by the NSMC FY Satellite Data Center; they can be downloaded from <http://fy3.satellite.cma.gov.cn/portalsite/default.aspx?currentculture=en-US>. The meteorological and radiation data from national stations were provided by the China Meteorological Data Center and are available at http://cdc.cma.gov.cn/cdc_en/home.dd. The ground observations were contributed by the Environmental and Ecological Science Data Center for West China (<http://westdc.westgis.ac.cn>). MODIS data were downloaded from the NASA Goddard Space Flight Center (GSFC) Distributed Active Archive Center (GDAAC) and can be found at <http://reverb.echo.nasa.gov/reverb/>.

Author Contributions: Bingfang Wu, Shufu Liu, Weiwei Zhu conceived and designed the experiments; Weiwei Zhu wrote the manuscript and Bingfang Wu revised the manuscript; Nana Yan, Qiang Xing and Shen Tan provided some useful advice for the study.

Conflicts of Interest: The authors declare no conflict of interest.

References

1. De, P.; Lima, E.; Sedyiyama, G.C.; da Silva, B.B.; Gleriani, J.M.; Soares, V.P. Seasonality of net radiation in two sub-basins of Paracatu by the use of MODIS sensor products. *Eng. Agric.* **2012**, *32*, 1184–1196.
2. Liu, G.S.; Liu, Y.; Xu, D. Comparison of evapotranspiration temporal scaling methods based on lysimeter measurements. *J. Remote Sens.* **2011**, *15*, 270–280.
3. Liu, G.; Liu, Y.; Hafeez, M.; Xu, D.; Vote, C. Comparison of two methods to derive time series of actual evapotranspiration using eddy covariance measurements in the southeastern Australia. *J. Hydrol.* **2012**, *454–455*, 1–6. [[CrossRef](#)]
4. Liu, G.; Hafeez, M.; Liu, Y.; Xu, D.; Vote, C. A novel method to convert daytime evapotranspiration into daily evapotranspiration based on variable canopy resistance. *J. Hydrol.* **2012**, *414–415*, 278–283. [[CrossRef](#)]
5. Suttles, J.T.; Ohring, G. Surface radiation budget for climate applications. *NASA Ref. Publ.* **1986**, *1169*, 1–123.
6. Ramanathan, V. The role of Earth radiation budget studies in climate and general circulation research. *J. Geophys. Res.* **1987**, *92*, 4075–4095. [[CrossRef](#)]
7. Zhou, X.; Tang, B.; Wu, H.; Li, Z. Estimating net surface longwave radiation from net surface shortwave radiation for cloudy skies. *Int. J. Remote Sens.* **2013**, *34*, 8104–8117. [[CrossRef](#)]
8. Liang, S. Narrowband to broadband conversions of land surface albedo I: Algorithms. *Remote Sens. Environ.* **2001**, *76*, 213–238. [[CrossRef](#)]
9. Angstrom, A. Solar and terrestrial radiation. Report to the international commission for solar research on actinometric investigations of solar and atmospheric radiation. *Q. J. R. Meteorol. Soc.* **1924**, *50*, 121–126. [[CrossRef](#)]
10. Swartman, R.K.; Ogunlade, O. Solar radiation estimates from common parameters. *Sol. Energy* **1967**, *11*, 170–172. [[CrossRef](#)]
11. Gariepy, J. *Estimation of Extra-Terrestrial Solar Radiation (Estimation du Rayonnement solaire Global)*; Internal Report, Service of Meteorology; Government of Quebec: Quebec City, QC, Canada, 1980.

12. Lewis, G. Estimates of irradiance over Zimbabwe. *Sol. Energy* **1983**, *31*, 609–612. [[CrossRef](#)]
13. Hargreaves, G.L.; Hargreaves, G.H.; Riley, J.P. Irrigation water requirements for the Senegal River Basin. *J. Irrig. Drain. Eng.* **1985**, *111*, 265–275. [[CrossRef](#)]
14. Bahel, V.; Bakhsh, H.; Srinivasan, R. A correlation for estimation of global solar radiation. *Energy* **1987**, *12*, 131–135. [[CrossRef](#)]
15. Ojosu, J.O.; Komolafe, L.K. Models for estimating solar radiation availability in south western Nigeria. *Niger. J. Sol. Energy* **1987**, *6*, 69–77.
16. Ododo, J.C.; Sulaiman, A.T.; Aidan, J.; Yuguda, M.M.; Ogbu, F.A. The importance of maximum air temperature in the parameterization of solar radiation in Nigeria. *Renew. Energy* **1995**, *6*, 751–763. [[CrossRef](#)]
17. Allen, R.G. Self-calibrating method for estimating solar radiation from air temperature. *J. Hydrol. Eng.* **1997**, *2*, 56–67. [[CrossRef](#)]
18. Supit, I.; van Kappel, R.R. A simple method to estimate global radiation. *Sol. Energy* **1998**, *63*, 147–160. [[CrossRef](#)]
19. Hussain, M.; Rahman, L.; Rahman, M.M. Techniques to obtain improved predictions of global radiation from sunshine duration. *Renew. Energy* **1999**, *18*, 263–275. [[CrossRef](#)]
20. Lin, W.; Lu, E. Validation of eight sunshine-based global radiation models with measured data at seven places in Yunnan Province, China. *Energy Convers. Manag.* **1999**, *40*, 519–525. [[CrossRef](#)]
21. Inci, T.T.; Emin, O. A study of estimating solar radiation in Elazig using geographical and meteorological data. *Energy Convers. Manag.* **1999**, *40*, 1577–1584.
22. Thornton, P.E.; Running, S.W. An improved algorithm for estimating incident daily solar radiation from measurements of temperature, humidity, and precipitation. *Agric. For. Meteorol.* **1999**, *93*, 211–228. [[CrossRef](#)]
23. Meza, F.; Varas, E. Estimation of mean monthly solar global radiation as a function of temperature. *Agric. For. Meteorol.* **2000**, *100*, 231–241. [[CrossRef](#)]
24. Muneer, T.; Gul, M.S. Evaluation of sunshine and cloud cover based models for generating solar radiation data. *Energy Convers. Manag.* **2000**, *41*, 461–482. [[CrossRef](#)]
25. Castellvi, F. A new simple method for estimating monthly and daily solar radiation. Performance and comparison with other methods at Lleida (NE Spain); a semiarid climate. *Theor. Appl. Climatol.* **2001**, *69*, 231–238. [[CrossRef](#)]
26. Winslow, J.C.; Hunt, E.R.; Piper, S.C. A globally applicable model of daily solar irradiance estimated from air temperature and precipitation data. *Ecol. Model.* **2001**, *143*, 227–243. [[CrossRef](#)]
27. Irmak, S.; Irmak, A.; Jones, J.W.; Howell, T.A.; Jacobs, J.M.; Allen, R.G.; Hoogenboom, G. Predicting daily net radiation using minimum climatological data. *J. Irrig. Drain. Eng.* **2003**, *129*, 256–269. [[CrossRef](#)]
28. El-Metwally, M. Simple new methods to estimate global solar radiation based on meteorological data in Egypt. *Atmos. Res.* **2004**, *69*, 217–239. [[CrossRef](#)]
29. Almorox, J.; Hontoria, C. Global solar radiation estimation using sunshine duration in Spain. *Energy Convers. Manag.* **2004**, *45*, 1529–1535. [[CrossRef](#)]
30. Chen, R.; Ersi, K.; Yang, J.; Lu, S.; Zhao, W. Validation of five global radiation models with measured daily data in China. *Energy Convers. Manag.* **2004**, *45*, 1759–1769. [[CrossRef](#)]
31. Rensheng, C.; Shihua, L.; Ersi, K.; Jianping, Y.; Xibin, J. Estimating daily global radiation using two types of revised models in China. *Energy Convers. Manag.* **2006**, *47*, 865–878. [[CrossRef](#)]
32. Chen, R.; Kang, E.; Ji, X.; Yang, J.; Zhang, Z. Trends of the global radiation and sunshine hours in 1961–1998 and their relationships in China. *Energy Convers. Manag.* **2006**, *47*, 2859–2866. [[CrossRef](#)]
33. Chen, R.; Kang, E.; Lu, S.; Yang, J.; Ji, X.; Zhang, Z.; Zhang, J. New methods to estimate global radiation based on meteorological data in China. *Energy Convers. Manag.* **2006**, *47*, 2991–2998. [[CrossRef](#)]
34. Jin, Z.; Wu, Y.; Gang, Y. General formula for estimation of monthly average daily global solar radiation in China. *Energy Convers. Manag.* **2005**, *46*, 257–268. [[CrossRef](#)]
35. Kadir, B. Correlations for estimation of daily global solar radiation with hours of bright sunshine in Turkey. *Energy* **2009**, *34*, 485–501.
36. Wu, W.; Tang, X.P.; Yang, C.; Guo, N.J.; Liu, H.B. Spatial estimation of monthly mean daily sunshine hours and solar radiation across mainland China. *Renew. Energy* **2013**, *57*, 546–553. [[CrossRef](#)]
37. Zhao, N.; Zeng, X.; Han, S. Solar radiation estimation using sunshine hour and air pollution index in China. *Energy Convers. Manag.* **2013**, *76*, 846–851. [[CrossRef](#)]

38. Yang, K.; Huang, G.W.; Tamai, N. A hybrid model for estimating global solar radiation. *Sol. Energy* **2001**, *70*, 13–22. [[CrossRef](#)]
39. Power, H.C. Estimating clear-sky beam irradiation from sunshine duration. *Sol. Energy* **2001**, *71*, 217–224. [[CrossRef](#)]
40. Tiba, C. Solar radiation in the Brazilian northeast. *Renew. Energy* **2001**, *22*, 565–578. [[CrossRef](#)]
41. Trnka, M.; Žalud, Z.; Eitzinger, J.; Dubrovský, M. Global solar radiation in Central European lowlands estimated by various empirical formulae. *Agric. For. Meteorol.* **2005**, *131*, 54–76. [[CrossRef](#)]
42. Yohanna, J.K.; Itodo, I.N.; Umogbai, V.I. A model for determining the global solar radiation for Makurdi, Nigeria. *Renew. Energy* **2011**, *36*, 1989–1992. [[CrossRef](#)]
43. Li, M.; Tang, X.; Wu, W.; Liu, H. General models for estimating daily global solar radiation for different solar radiation zones in mainland China. *Energy Convers. Manag.* **2013**, *70*, 139–148. [[CrossRef](#)]
44. Ertekin, C.; Yaldiz, O. Comparison of some existing models for estimating global solar radiation for Antalya (Turkey). *Energy Convers. Manag.* **2000**, *41*, 311–330. [[CrossRef](#)]
45. Robaa, S.M. Validation of the existing models for estimating global solar radiation over Egypt. *Energy Convers. Manag.* **2009**, *50*, 184–193. [[CrossRef](#)]
46. Wu, B.F.; Liu, S.F.; Zhu, W.W.; Yu, M.Z.; Yan, N.N.; Xing, Q. A method to estimate sunshine duration using cloud classification data from a geostationary meteorological satellite (FY-2D) over the Heihe River Basin. *Sensors* **2016**, *16*, 1859. [[CrossRef](#)] [[PubMed](#)]
47. Allen, R.G.; Pereira, L.S.; Raes, D.; Smith, M. *Crop Evapotranspiration: Guidelines for Computing Crop Water Requirements*; Irrigation and Drainage Paper 56; FAO: Rome, Italy, 1998.
48. Ertekin, C.; Evrendilek, F. Spatio-temporal modeling of global solar radiation dynamics as a function of sunshine duration for Turkey. *Agric. For. Meteorol.* **2007**, *145*, 36–47. [[CrossRef](#)]
49. Tian, H. Remote-Sensed Estimates of Evapotranspiration over a Complex Terrain of the Inland Hei River Basin. Ph.D. Dissertation, Cold and Arid Regions Environment and Engineering Research Institute, Academy of Sciences, Lanzhou, China, June 2008. (In Chinese)
50. Huang, C.; Li, Y.; Gu, J. Improving Estimation of Evapotranspiration under Water-Limited Conditions Based on SEBS and MODIS Data in Arid Regions. *Remote Sens.* **2015**, *7*, 16795–16814. [[CrossRef](#)]
51. Chelbi, M.; Gagnon, Y.; Waewsak, J. Solar radiation mapping using sunshine duration-based models and interpolation techniques: Application to Tunisia. *Energy Convers. Manag.* **2015**, *101*, 203–215. [[CrossRef](#)]
52. Matsui, H.; Osawa, K. Calibration effects of the net longwave radiation equation in penman-type methods at Tateno, Japan. *Hydrol. Res. Lett.* **2015**, *9*, 113–117. [[CrossRef](#)]
53. Jensen, M.E.; Burman, R.D.; Allen, R.G. *Evapotranspiration and Irrigation Water Requirements*; ASCE Manual 70; American Society of Civil Engineers: New York, NY, USA, 1990.
54. Yin, Y.; Wu, S.; Zheng, D.; Yang, Q. Radiation calibration of FAO56 Penman-Monteith model to estimate reference crop evapotranspiration in China. *Agric. Water Manag.* **2008**, *95*, 77–84. [[CrossRef](#)]
55. Kjaersgaard, J.H.; Cuenca, R.H.; Martinez-Cob, A.; Gavilan, P.; Plauborg, F.; Mollerup, M.; Hansen, S. Comparison of the performance of net radiation calculation models. *Theor. Appl. Climatol.* **2009**, *98*, 57–66. [[CrossRef](#)]
56. Zhu, W.; Wu, B.; Yan, N.; Feng, X.; Xing, Q. A method to estimate diurnal surface soil heat flux from MODIS data for a sparse vegetation and bare soil. *J. Hydrol.* **2014**, *511*, 139–150. [[CrossRef](#)]
57. Gao, Y.; Hu, Y. *Advances in HEIFE Research (1987–1994)*, 1st ed.; Special Issue; China Meteorological: Beijing, China, 1994.
58. Annai, M. *Remote Sensing Information Model*; Peking University Press: Beijing, China, 1997.
59. Ma, Y.; Dai, Y.; Ma, W.; Li, M.; Wang, J.; Wen, J.; Sun, F. Satellite remote sensing parameterization of regional land surface heat fluxes over heterogeneous surface of arid and semi-arid areas. *Plateau Meteorol.* **2004**, *23*, 139–146.
60. Ma, Y.M.; Ma, W.Q.; Li, M.S.; Sun, F.L.; Wang, J.M. Remote sensing parameterization of land surface heat fluxes over the middle reaches of the Heihe river. *J. Desert Res.* **2004**, *24*, 392–401.
61. Li, X.; Li, X.; Li, Z.; Ma, M.; Wang, J.; Xiao, Q.; Liu, Q.; Che, T.; Chen, E.; Yan, G.; et al. Watershed allied telemetry experimental Research. *J. Geophys. Res.* **2009**, *114*, D22103. [[CrossRef](#)]
62. Li, X.; Cheng, G.; Liu, S.; Xiao, Q.; Ma, M.; Jin, R.; Che, T.; Liu, Q.; Wang, W.; Qi, Y.; et al. Heihe watershed allied telemetry experimental Research (HiWATER): Scientific objectives and experimental design. *Bull. Am. Meteorol. Soc.* **2013**, *94*, 1145–1160. [[CrossRef](#)]

63. Ackerman, S.; Strabala, K.; Menzel, P.; Frey, R.; Moeller, C.; Gumley, L.; Baum, B.; Seemann, S.W.; Zhang, H. Discriminating Clear-Sky from Cloud with MODIS Algorithm. Available online: http://library.ssec.wisc.edu/research_Resources/publications/pdfs/SSECPUBS/SSEC_Publication_No_06_10_A1.pdf (accessed on 3 January 2017).
64. Wang, Y.; Li, X.; Tang, S. Validation of the SEBS-derived sensible heat for FY3A/VIRR and TERRA/MODIS over an alpine grass region using las measurements. *Int. J. Appl. Earth Obs.* **2013**, *23*, 226–233. [CrossRef]
65. Xu, J.M. Development and trend of China meteorological satellite. *Sci. Technol. Rev.* **2010**, *28*, 3–13.
66. Xu, J.M. Chinese meteorological satellites, achievements and applications. *Meteorol. Mon.* **2010**, *36*, 94–100.
67. Qian, Q.J.; Wu, B.F.; Xiong, J. Interpolation system for generating meteorological surfaces using to compute evapotranspiration in Haihe River Basin. In Proceedings of the IEEE International Geoscience and Remote Sensing Symposium, Milan, Italy, 26–31 July 2005; pp. 616–619.
68. Prescott, J.A. Evaporation from a water surface in relation to solar radiation. *Trans. R. Soc. Sci.* **1940**, *64*, 114–225.
69. Revfeim, K. On the relationship between radiation and mean daily sunshine. *Agric. For. Meteorol.* **1997**, *86*, 183–191. [CrossRef]
70. Brunt, D. Notes on radiation in the atmosphere. I. *Q. J. R. Meteorol. Soc.* **1932**, *58*, 389–420. [CrossRef]
71. Penman, H.L. Natural evaporation from open water, bare soil and grass. *Proc. R. Soc. A* **1948**, *193*, 120–145. [CrossRef]
72. Bastiaanssen, W.G.M. Regionalization of Surface Flux Densities and Moisture Indicators in Composite Terrain: A Remote Sensing Approach under Clear Skies in Mediterranean Climates. Ph.D. Dissertation, Wageningen Agricultural University, Wageningen, The Netherlands, 1995.
73. Levenberg, K. A method for the solution of certain nonlinear problems in least squares. *Q. Appl. Math.* **1944**, *2*, 164–168. [CrossRef]
74. Nash, J.E.; Sutcliffe, J.V. River flow forecasting through conceptual models part I—A discussion of principles. *J. Hydrol.* **1970**, *10*, 282–290. [CrossRef]
75. Cai, J.; Liu, Y.; Lei, T.; Pereira, L.S. Estimating reference evapotranspiration with the FAO Penman-Monteith equation using daily weather forecast messages. *Agric. For. Meteorol.* **2007**, *145*, 22–35. [CrossRef]
76. Legates, D.R.; McCabe, G.J. Evaluating the use of “goodness-of-fit” measures in hydrologic and hydroclimatic model validation. *Water Resour. Res.* **1999**, *35*, 233–241. [CrossRef]
77. Fox, D.G. Judging air quality model performance. *Bull. Am. Meteorol. Soc.* **1981**, *62*, 599–609. [CrossRef]
78. Willmott, C.J. Some comments on the evaluation of model performance. *Bull. Am. Meteorol. Soc.* **1982**, *63*, 1309–1313. [CrossRef]
79. Isaaks, E.H.; Srivastava, R.M. *An Introduction to Applied Geostatistics*; Oxford University Press: New York, NY, USA, 1989.



© 2017 by the authors; licensee MDPI, Basel, Switzerland. This article is an open access article distributed under the terms and conditions of the Creative Commons Attribution (CC-BY) license (<http://creativecommons.org/licenses/by/4.0/>).